Neuro-Oncology

Neuro-Oncology 17(6), 810–821, 2015
doi:10.1093/neuonc/nou305
Advance Access date 4 November 2014

Disulfiram modulates stemness and metabolism of brain tumor initiating cells in atypical teratoid/rhabdoid tumors

Seung Ah Choi†, Jung Won Choi†, Kyu-Chang Wang, Ji Hoon Phi, Ji Yeoun Lee, Kyung Duk Park, Dayoung Eum, Sung-Hye Park, Il Han Kim, and Seung-Ki Kim

Division of Pediatric Neurosurgery, Pediatric Clinical Neuroscience Center, Seoul National University Children's Hospital, Seoul, Republic of Korea (S.A.C., J.W.C., K.-C.W., J.H.P., J.Y.L., D.E., S.-K.K.); Adolescent Cancer Center, Seoul National University Cancer Hospital, Seoul, Republic of Korea (S.A.C., J.W.C., J.H.P., J.Y.L., K.D.P., D.E., S.-K.K.); Department of Pediatrics, Seoul National University Children's Hospital, Seoul, Republic of Korea (K.D.P.); Department of Pathology, Seoul National University Children's Hospital, Seoul, Republic of Korea (S-H.P.); Department of Radiation Oncology, Seoul National University Hospital, Seoul National University College of Medicine, Seoul, Republic of Korea (I.H.K.)

Corresponding Author: Seung-Ki Kim, MD, PhD, Division of Pediatric Neurosurgery, Seoul National University Children's Hospital, 101 Daehak-ro, Jongno-gu, Seoul 110–744, Republic of Korea (nsthomas@snu.ac.kr).

†These authors contributed equally to this work.

Background. Atypical teratoid/rhabdoid tumors (AT/RT) are among the most malignant pediatric brain tumors. Cells from brain tumors with high aldehyde dehydrogenase (ALDH) activity have a number of characteristics that are similar to brain tumor initiating cells (BTICs). This study aimed to evaluate the therapeutic potential of ALDH inhibition using disulfiram (DSF) against BTICs from AT/RT.

Methods. Primary cultured BTICs from AT/RT were stained with Aldefluor and isolated by fluorescence activated cell sorting. The therapeutic effect of DSF against BTICs from AT/RT was confirmed in vitro and in vivo.

Results. AT/RT cells displayed a high expression of ALDH. DSF demonstrated a more potent cytotoxic effect on $ALDH^+$ AT/RT cells compared with standard anticancer agents. Notably, treatment with DSF did not have a considerable effect on normal neural stem cells or fibroblasts. DSF significantly inhibited the ALDH enzyme activity of AT/RT cells. DSF decreased self-renewal ability, cell viability, and proliferation potential and induced apoptosis and cell cycle arrest in $ALDH^+$ AT/RT cells. Importantly, DSF reduced the metabolism of $ALDH^+$ AT/RT cells by increasing the nicotinamide adenine dinucleotide ratio of NAD^+/NADH and regulating Silent mating type Information Regulator 2 homolog 1 (SIRT1), nuclear factor-kappaB, Lin28A/B, and miRNA let-7g. Animals in the DSF-treated group demonstrated a reduction of tumor volume ($P < .05$) and a significant survival benefit ($P = .02$).

Conclusion. Our study demonstrated the therapeutic potential of DSF against BTICs from AT/RT and suggested the possibility of ALDH inhibition for clinical application.

Keywords: aldehyde dehydrogenase, atypical teratoid/rhabdoid tumors, brain tumor initiating cells, disulfiram, sirtuin.

Atypical teratoid/rhabdoid tumors (AT/RT) are among the most malignant pediatric brain tumors.[1] Although AT/RT are an uncommon disease, the incidence in children under 3 years of age is remarkably high, up to 20% of malignant brain tumors.[2] This high prevalence of AT/RT in young children may lead to a poor prognosis due to limited treatment options. To improve outcomes, many clinical studies have been attempted, including high dose chemotherapy with autologous stem cell rescue,[3] early radiation therapy,[2] and proton therapy.[4] However, there is no optimal treatment regimen for AT/RT to date, making AT/RT a rarely curable disease.

Brain tumor initiating cells (BTICs) are a type of cancer stem cell (CSC), retaining stem cell–like properties.[5] Recent studies revealed that these BTICs and chemo- or radioresistance are closely interrelated, even though BTICs represent a small percentage of the tumor cell population.[6]

Aldehyde dehydrogenase (ALDH) is a polymorphic enzyme responsible for the oxidation of aldehydes to carboxylic acids, and this reaction is dependent on nicotinamide adenine dinucleotide (NAD^+), producing NADH. ALDH activity, which can be easily measured using an Aldefluor assay, is now used as one of the CSC markers for many cancers.[7,8] We previously reported

Received 21 February 2014; accepted 1 October 2014

that primary brain tumors contain distinct subpopulations of cells that have high expression levels of ALDH and BTIC characteristics.[8] In that study, the ALDH$^+$ fraction tended to be higher in aggressive tumors, such as AT/RT. Furthermore, we found that the targeted knockdown of ALDH1 by short hairpin RNA in BTICs potently disrupted their self-renewing ability.[8]

Disulfiram (DSF) has been used for decades to treat alcoholism by preventing the conversion of acetaldehyde to acetic acid to irreversibly inhibit ALDH, causing an unpleasant reaction when alcohol is consumed.[9] We estimated that DSF might have tumor suppressive effects because DSF inhibits ALDH, which is abundant in CSCs. Indeed, it has been widely reported that DSF has a tumor control effect on several human cancers, such as breast cancer,[10] colorectal cancer,[11] and brain tumors.[12,13] However, DSF treatment for AT/RT, which has a high expression of ALDH, has not been investigated.

This study aimed to evaluate the therapeutic potential of ALDH inhibition using DSF, particularly against BTICs within AT/RT, through both in vitro and in vivo experiments. Furthermore, we proposed the possible mechanism of DSF treatment in AT/RT.

Materials and Methods

Cell Cultures

Atypical teratoid/rhabdoid tumor tissue samples were obtained from 2 pediatric patients (a 1-mo-old boy, SNU.AT/RT-1; and a 1-y-old boy, SNU.AT/RT-2), the same tumor cells used in our previous study.[8] They did not receive neoadjuvant therapies. Their parents provided written informed consent approved by the institutional review board of the Seoul National University Hospital. Both tumors were negative for protein expression of INI-1/SMARCB1 (integrase interactor 1/Switch sucrose nonfermentable related, matrix associated, actin dependent regulator of chromatin, subfamily B) and fulfilled the criteria of AT/RT. Within 4 h after surgical removal, the tumor cells were isolated and maintained as described previously.[14] All experiments were conducted before the fourth cell passage. HB1.F3 neural stem cells (NSCs) were obtained from Chung-Ang University, Seoul. AT/RT cell lines (CRL-3020 and CRL-3036) and the human foreskin fibroblast 1 (HFF1) cell line was purchased from American Type Culture Collection. AT/RT cell lines (BT-12 and BT-16) were obtained from Dr Peter Houghton (Nationwide Children's Hospital). (For cell line cultures, see Supplementary Materials.) All in vitro experiments were repeated 3 times in triplicate.

Aldehyde Dehydrogenase Activity Analysis and Fluorescence Activated Cell Sorting

Freshly dissociated tumor spheres were analyzed using an Aldefluor assay kit (Aldagen) and detected as described previously.[8] For further studies, ALDH$^+$ and ALDH$^-$ AT/RT cells were sorted using a FACSAria flow cytometer (BD Biosciences). After DSF treatment at the 50% inhibitory concentration (IC_{50}), we confirmed ALDH activity as described above.

Tumor Sphere Characterization

For characterization, spheroid ALDH$^+$ AT/RT cells were plated on extracellular matrix (Sigma-Aldrich)–coated 8-well Lab-Tek chamber slides (Nunc) for 1 h. Then the cells were stained with primary antibodies directed against nestin (1:200; Chemicon) or Musashi (1:100; Neuromics) by immunofluorescent staining, and images were obtained using a Zeiss confocal microscope.

Cell Viability Assay

Disulfiram, ifosfamide (IFO), carboplatin, and etoposide were purchased from Sigma-Aldrich. Drugs were dissolved in dimethyl sulfoxide (DMSO; Sigma-Aldrich). Cellular viability was measured using the Cell Counting Kit 8 (Dojindo Molecular Technologies). ALDH$^+$ AT/RT cells (5×10^3 cells/well) were seeded in 96-well plates. After 24 h, the different drug solutions were added and incubated for 72 h. The data were averaged and normalized against the untreated control (DMSO) samples. For further studies, cells were treated with the IC_{50} values of DSF and/or IFO (Supplementary Table S1. For combination treatment of DSF + IFO or radiotherapy, see Supplementary Materials).

Sphere-Forming Assay and Limiting Dilution Assay

To generate tumor spheres, ALDH$^+$ AT/RT cells (1×10^3) were cultured onto 48-well ultra-low cluster plates (Costar) in neurosphere basal medium for 3 days. To determine the effect of DSF on tumor sphere formation, spheres were dissociated into single cells using Accutase (Invitrogen) and mechanical disruption. After washing, the cells (1×10^3) were seeded in 6-well plates and treated for 48 h. The tumor spheres with diameters >20 μm were counted under an inverted microscope (Leica Microsystems). Limiting dilution assay was performed as described previously.[8]

5-Ethynyl-2′-Deoxyuridine and TUNEL Staining, Annexin V, and Cell Cycle Analysis

For staining for 5-ethynyl-2′-deoxyuridine (EdU) or terminal deoxynucleotidyl transferase deoxyuridine triphosphate nick end labeling (TUNEL), the dissociated ALDH$^+$ AT/RT cells (1×10^4) were labeled using the Click-iT EdU assay kit (Invitrogen) for proliferation and Click-iT TUNEL assay kit (Invitrogen) for apoptosis. An annexin V assay was performed using an annexin V–fluorescein isothiocyanate kit (BD Biosciences) and propidium iodide (PI) to detect apoptotic cells. The cells (1×10^5) were treated according to the manufacturer's protocol and analyzed by fluorescence activated cell sorting (FACS; FACSCalibur, BD Biosciences). CellQuest Pro software (BD Biosciences) and ModFit LT software (Verity Software House) were used to determine the distribution of apoptotic cells. The proliferative or apoptotic ratio was calculated by plotting the EdU- or TUNEL-positive cell number against the total cell number. (For cell cycle analysis, see Supplementary Materials.)

NAD^+/NADH Quantification Assay

The NAD^+/NADH ratio was measured using a BioVision NAD^+/NADH quantification assay kit in the ALDH$^+$ AT/RT cells treated after 24 h according to the manufacturer's instructions. To

calculate the NAD^+ and NADH concentrations, a standard curve generated with known amounts of purified NADH was used.

Real-time Quantitative Polymerase Chain Reaction

Total RNA was extracted from cells using the Pure Link RNA Kit (Invitrogen). Real-time quantitative PCR assays were performed using a TaqMan miRNA assay (Applied Biosystems) and the ABI 7500 Sequence Detection System. Gene-specific reverse transcription for miR-let7g (002118) and RUN6B (001093), using ~0.2 μg of purified total RNA, was used to detect miRNA levels. The target miRNA abundance in each sample was normalized to its reference RUN6B. The relative expression levels in each sample were calculated and quantified by using the $2^{-\Delta\Delta Ct}$ method. The value of each control sample was set to one and was used to calculate the fold change of the target.

Western Blot Analysis

After $ALDH^+$ AT/RT cells were treated for 36 h, western blot analysis was performed as previously reported.[8] The membranes were blotted with the following antibodies: anti–silent mating type information regulation 2 homolog 1 (SIRT1; 1:1000; Abcam), anti–nuclear factor-kappaB (NF-κB; 1:500; Abcam), anti-Lin28A (1:500; Thermo Scientific), anti-Lin28B (1:200; Abcam), anti–signal transducer and activator of transcription 3 (STAT3; 1:1000; Cell Signaling), anti-phospho-STAT3 (pSTAT3; 1:1000; Cell Signaling), anti-Akt (1:1000; Cell Signaling), anti-phospho-Akt (pAkt; 1:1000; Cell Signaling), and anti–β-actin (1:10 000; Sigma- Aldrich). The blot was incubated with a horseradish peroxidase–conjugated species-specific secondary antibody (1:5000; Jackson Laboratory). The blots were detected as described previously.[8] Band density was analyzed using ImageJ software (National Institutes of Health). The values indicate protein level normalized to its corresponding β-actin levels.

Intracranial Orthotopic Mouse Model

Animal experiments were approved by the animal facility of the Seoul National Institutional Animal Care and Use Committee in accordance with national and institutional guidelines. The protocol was also compliant with national regulatory standards.

Seven-week-old female Bagg Albino/c nude mice (OrientBio) were anesthetized with an intramuscular injection of a solution of 30 mg/kg Zoletil (Virbac) and 10 mg/kg xylazine (Bayer Korea). AT/RT spheroid cells were injected stereotactically into the brains using a stereotactic device (1 mm anterior and 2 mm lateral to the bregma, 3 mm depth from the dura).

In vivo Short-term Therapeutic Efficacy of Disulfiram

Seven days after the implantation of AT/RT spheroid cells (1×10^5), the animals were randomized into 2 groups: DMSO control and DSF 100 mg/kg, and were administered drugs i.p. for 5 consecutive days, followed by a 2-day resting period as one cycle. For tumor volume analysis, the animals received 3 cycles of chemotherapy ($n = 5$ for each group). At 28 days after AT/RT spheroid cell implantation, the animals were perfused with 4% paraformaldehyde. The brain tissues were embedded in an optimum cutting temperature compound (Tissue-Tek) for frozen sectioning and stored at −80°C. The brains were then sectioned at 10 μm and stained with hematoxylin and eosin. The tumor volume was recorded using the formula for an ellipsoid as described previously.[14]

Sectioned brain tissues used for histological analysis and the description are detailed in Supplementary Materials.

In vivo Long-term Therapeutic Efficacy of Disulfiram

For long-term survival analysis, after implantation of AT/RT spheroid cells (1×10^4), the animals were randomized into 4 groups: DMSO control, DSF 100 mg/kg, IFO 100 mg/kg, and DSF with IFO. We added another group in which animals received DSF without tumor cell implantation for safety. The animals received 5 cycles of chemotherapy ($n = 10$ for each group) and were followed until they died or for a maximum of 150 days, at which time the animals were sacrificed. Discomfort or distress was assessed by animal care personnel with no knowledge of the protocol design. All euthanized animals were verified as bearing tumors by necropsy. The endpoint for the therapeutic study was long-term survival.

Statistical Analyses

All values were calculated as mean ± SD or expressed as a percentage ± SD of controls. Multiple group comparisons were performed by 1-way ANOVA with a post hoc test. Differences between 2 groups were determined using a 2-tailed Student's *t*-test. Multiparameter statistics for the Kaplan–Meier survival curves were performed by a log-rank test. GraphPad Prism software was used for all analyses. Differences were considered statistically significant at $P < .05$.

Results

Isolation, Aldehyde Dehydrogenase Activity Analysis, and Characterization of Atypical Teratoid/Rhabdoid Tumor Cells

We successfully isolated spheroid cells from 2 different AT/RT tissues (SNU.AT/RT-1 and SNU.AT/RT-2). We identified the distribution of $ALDH^+$ cells in AT/RT spheroid cells by FACS analysis to determine ALDH enzyme activity. Spheroid cells from both AT/RT tissues contained a high level of $ALDH^+$ cells (SNU.AT/RT-1: 28.8% ± 9.2% and SNU.AT/RT-2: 18.2% ± 7.2%; Fig. 1A). The primary cultured AT/RT spheroid cells highly expressed both nestin and Musashi (Fig. 1B).

We identified the distribution of $ALDH^+$ cells in 4 established cell lines. The cells contained a few $ALDH^+$ cells (CRL-3020: 1.1% ± 0.5%, CRL-3036: 0.9% ± 0.7%, BT-12: 0.8% ± 0.6%, and BT-16: 0.2% ± 0.1%; Supplementary Fig. S1A).

Effects of Disulfiram on the Cell Viability of $ALDH^+$ AT/RT cells

To compare the anticancer effect of DSF on cell viability with the effects of standard anticancer drugs, we treated 2 $ALDH^+$ AT/RT primary cells, 4 established AT/RT cell lines, NSCs (HB1.F3), and fibroblasts (HFF1) with DSF or several anticancer drugs. The IC_{50}

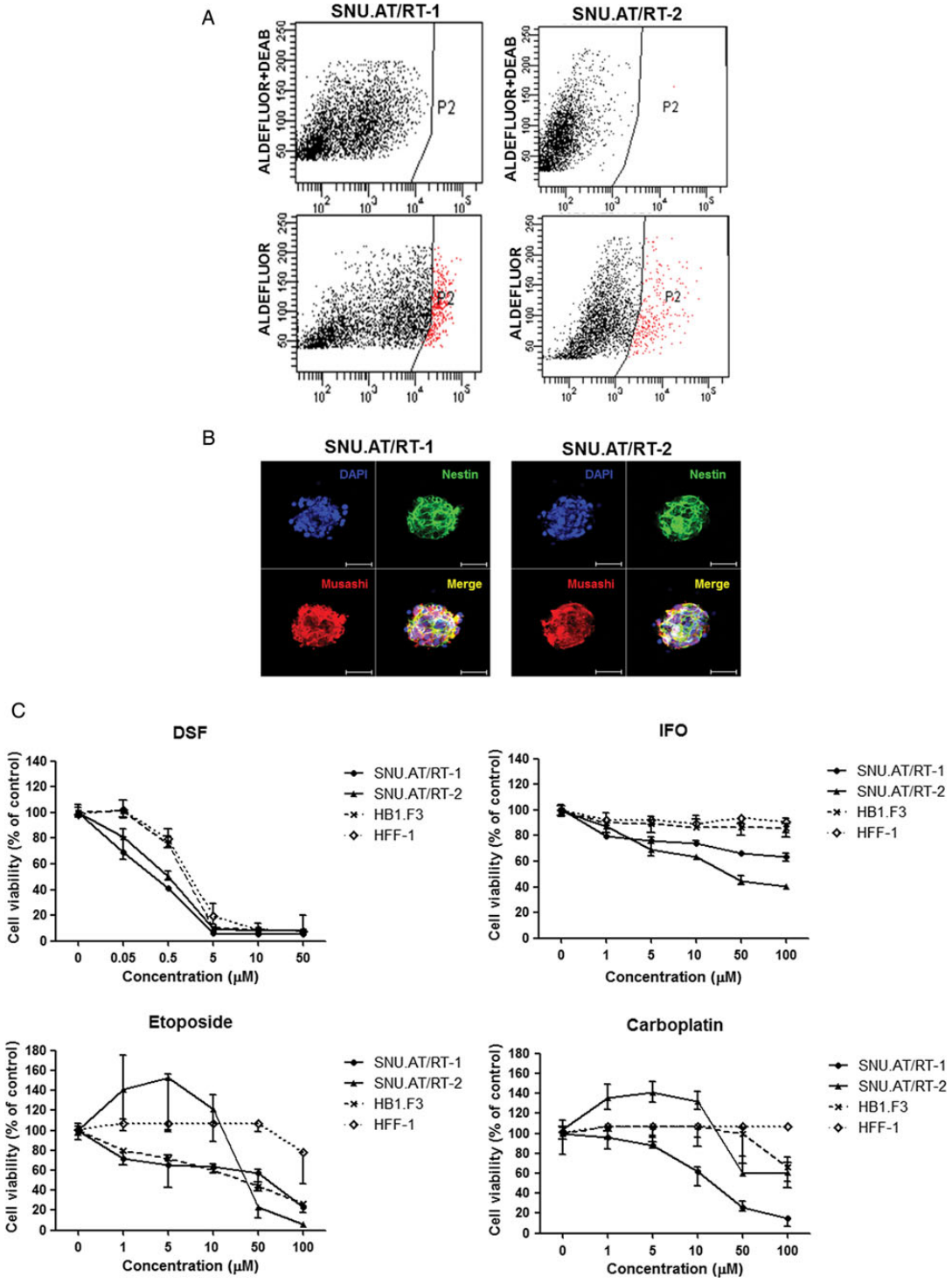

Fig. 1. ALDH activity analysis, characterization of AT/RT spheroid cells, and comparison of the chemosensitivity of ALDH$^+$ AT/RT cells with normal cells. (A) Flow cytometry analysis shows ALDH enzyme activities in both SNU.AT/RT-1 (28.8% ± 9.2%) and SNU.AT/RT-2 (18.2% ± 7.2%) cells. DEAB, diethylaminobenzaldehyde. (B) The expression of NSC markers determined by immunofluorescence staining with nestin (green) and Musashi (red) in SNU.AT/RT-1 and -2 cells. Scale bar, 50 μm. DAPI, 4′,6′-diamidino-2-phenylindole. (C) Cells were treated with increasing concentrations of DSF, IFO, carboplatin, and etoposide. Cell viability was decreased (IC_{50}: 0.07 ± 0.18 μM in SNU.AT/RT-1 and 0.61 ± 0.17 μM in SNU-AT/RT-2) in 2 different ALDH$^+$ AT/RT cells. DSF is more effective than the other drugs. Compared with ALDH$^+$ AT/RT cells, normal cells are more resistant to DSF. (D) Synergistic effect of DSF and IFO combination on cell viability (***$P < .001$ in both SNU.AT/RT-1 and SNU-AT/RT-1 cells). (E) Combination treatment with DSF and radiation. The combination treatment resulted in significant augmentation of cytotoxic effect in SNU.AT/RT-1 but not in SNU.ATRT-2 cells (***$P < .001$ in SNU.AT/RT-1 cells).

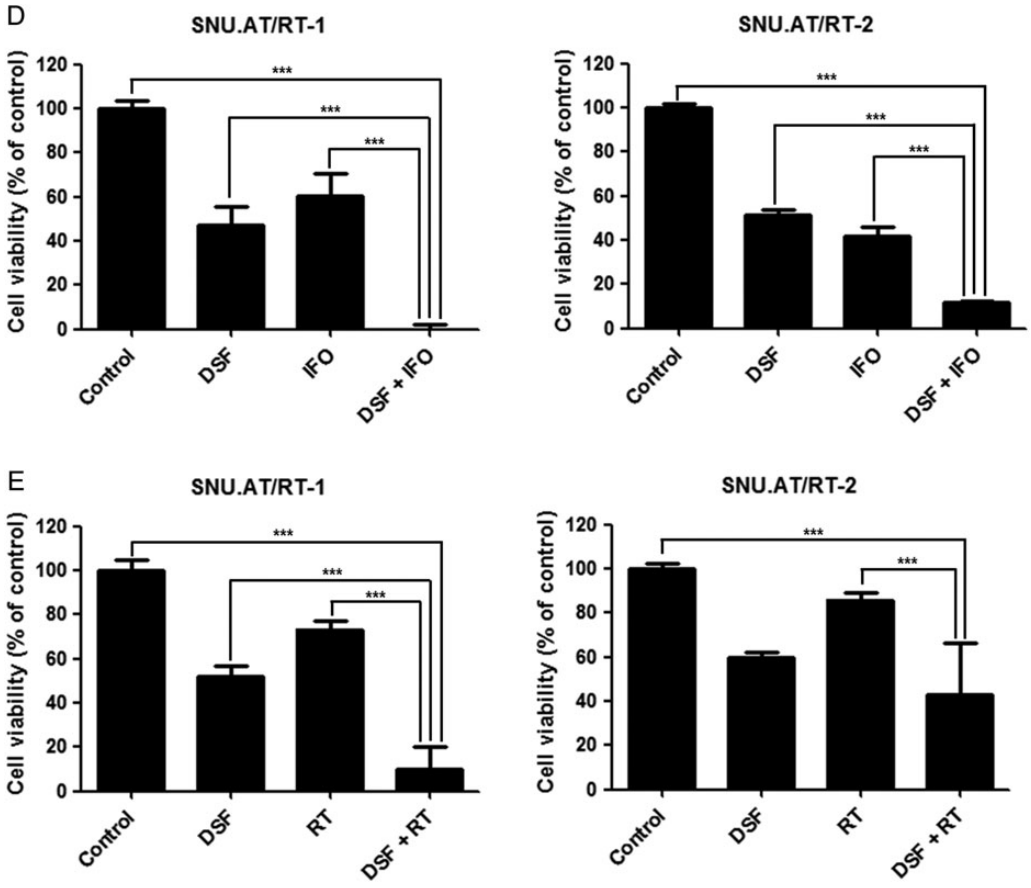

Fig. 1. *Continued*

value of the different chemotherapeutic agents was obtained from a dose-response curve at 72 h (Fig. 1C). Two different ALDH$^+$ AT/RT primary cells were more sensitive to DSF than other drugs (IC_{50} of DSF was 0.07 ± 0.18 μM for SNU.AT/RT-1 cells and 0.61 ± 0.17 μM for SNU.AT/RT-2 cells; Supplementary Table S1). Notably, both ALDH$^+$ AT/RT cells were not significantly affected by other anticancer drugs at physiologically achievable concentrations. Within the same concentration ranges, HB1.F3 and HFF1 cells were more resistant to DSF than ALDH$^+$ AT/RT cells (IC_{50} of DSF was 1.04 ± 0.10 μM for HB1.F3 cells and 1.51 ± 0.26 μM for HFF1 cells). We assessed the cell viability for 2 cell lines after treatment of DSF and obtained the IC_{50} value at 72 h.

Atypical teratoid/rhabdoid tumor cell lines were also sensitive to DSF (IC_{50} of DSF was 0.31 ± 0.02 μM for CRL-3020 cells and 0.25 ± 0.01 for CRL-3036 cells, 0.025 ± 0.008 μM for BT-12 cells, and 0.029 ± 0.005 for BT-16 cells; Supplementary Fig. S1B).

Combination Treatment With Disulfiram and Ifosfamide

The combination treatment with DSF and IFO significantly decreased the cell viability in AT/RT cells in vitro (control vs DSF + IFO: $100\% \pm 3.6\%$ vs $1.2\% \pm 2.1\%$, $P < .001$; DSF vs DSF + IFO: $47.9 \pm 7.8\%$ vs $1.2\% \pm 2.1\%$, $P < .001$; IFO vs DSF + IFO: 63.5% ±10.6 % vs $1.2\% \pm 2.1\%$, $P < .001$ in SNU.AT/RT-1; control vs DSF + IFO: $100\% \pm 1.7\%$ vs $11.9\% \pm 6.4\%$, $P < .001$; DSF vs DSF + IFO: $51.4\% \pm 7.2\%$ vs $11.9 \pm 6.4\%$, $P < .001$; IFO vs DSF + IFO: $40.3\% \pm 10.9\%$ vs $11.9\% \pm 6.4\%$, $P < .001$ in SNU.AT/RT-2; Fig. 1D).

Combination Treatment With Disulfiram and Radiation

When DSF was combined with radiotherapy, additive cytotoxicity was observed in SNU.AT/RT-1 cells compared with single treatment (control vs DSF + radiotherapy: $100\% \pm 5.1\%$ vs $9.8\% \pm 10.5\%$, $P < .001$; DSF vs DSF + radiotherapy: $51.9\% \pm 4.8\%$ vs $9.8\% \pm 10.5\%$, $P < .001$; radiotherapy vs DSF + radiotherapy: $73.2\% \pm 3.7\%$ vs $9.8\% \pm 10.5\%$, $P < .001$ in SNU.AT/RT-1; Fig. 1E). Although there was no significance between DSF single and DSF + radiation combination treatment in SNU.AT/RT-2 cells (control vs DSF + radiotherapy: $100\% \pm 2.4\%$ vs $34.6\% \pm 24.6\%$, $P < .001$; DSF vs DSF + radiotherapy: $59.7\% \pm 2.7\%$ vs $34.6\% \pm 24.6\%$, $P > .05$; radiotherapy vs DSF + radiotherapy: $85.9\% \pm 3.4\%$ vs $34.6\% \pm 24.6\%$, $P < .001$ in SNU.AT/RT-2; Fig. 1E), combination treatment might have an influential cytotoxic effect.

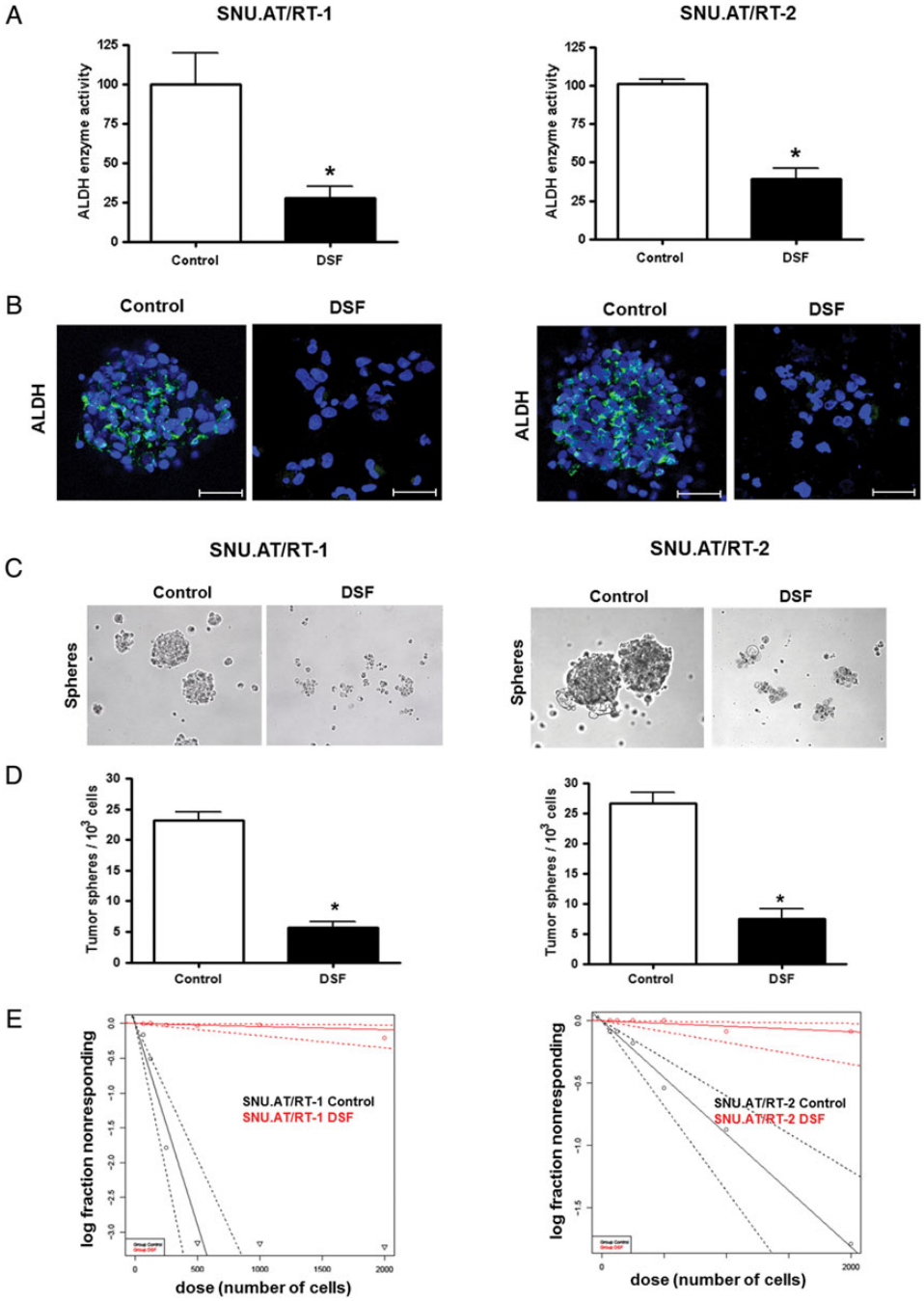

Fig. 2. Effect of DSF on ALDH$^+$ AT/RT cells. (A) DSF inhibits ALDH enzyme activity more than 60% (*$P < .05$ in SNU.AT/RT-1 and SNU.AT/RT-2). (B–D) DSF treatment decreases ALDH protein expression and sphere-forming ability (*$P < .05$ in both SNU.AT/RT-1 and SNU.AT/RT-2). (E) Limiting dilution analysis shows that DSF inhibits the self-renewal ability. Magnification, 20×. The cells were counterstained with DAPI (4′,6′-diamidino-2-phenylindole).

Inhibition of Aldehyde Dehydrogenase Enzyme Activity and Sphere-Forming Ability by Disulfiram

We confirmed the effect of DSF on ALDH enzyme activity using an Aldefluor assay and ALDH expression by immunofluorescence staining in AT/RT cells. DSF significantly decreased ALDH enzyme activity in AT/RT spheroid cells (control vs DSF-treated cells: 100% ± 40.5% vs 27.5% ± 15.2%, $P < .05$ in SNU.AT/RT-1 and 100% ± 6.0% vs 39.3% ± 13.5%, $P < .05$ in SNU.AT/RT-2; Fig. 3A) and the expression of the ALDH protein (Fig. 2B).

To determine self-renewal ability after DSF treatment in ALDH$^+$ AT/RT cells, we performed a tumor sphere formation

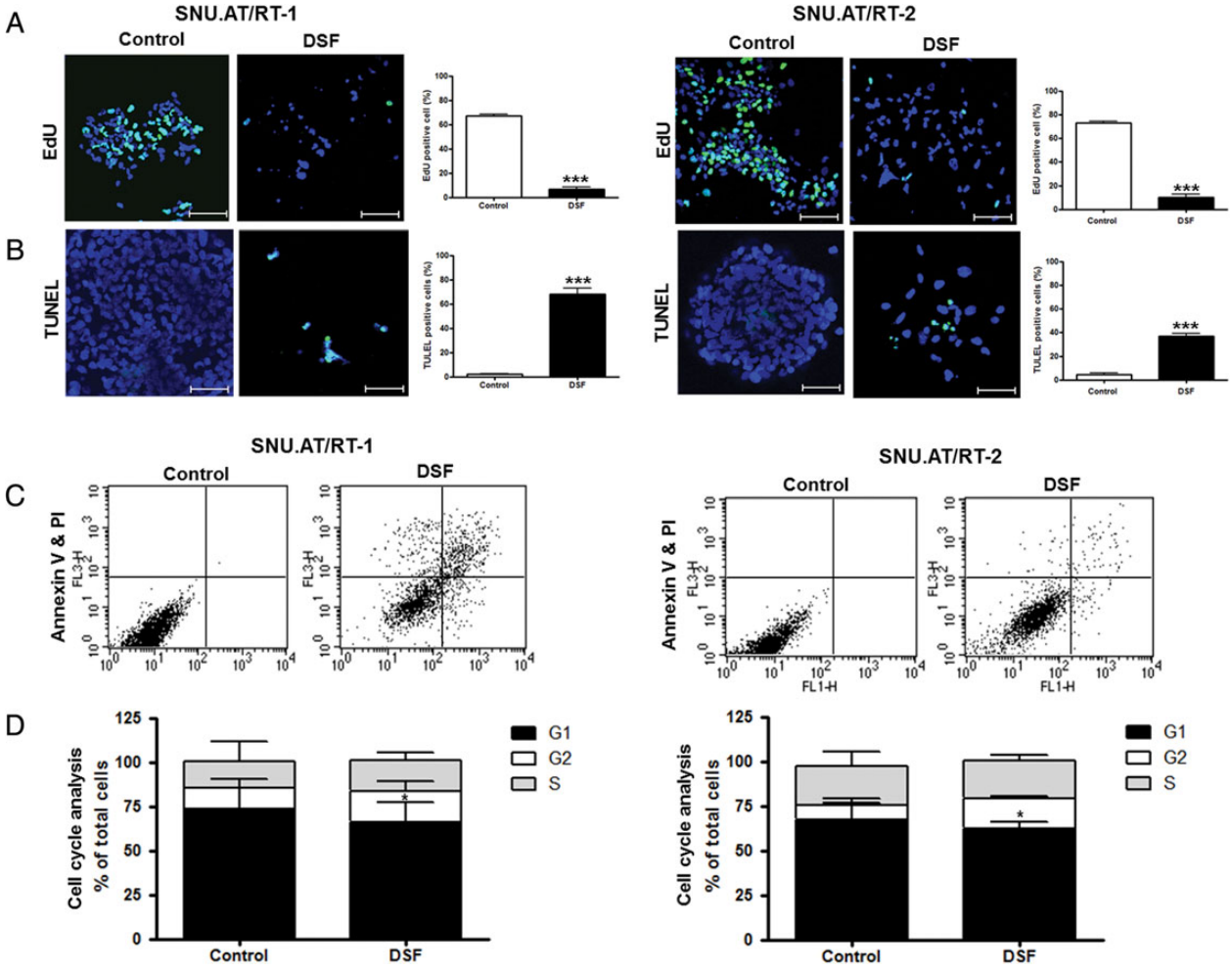

Fig. 3. Anticancer effect of DSF on ALDH$^+$ AT/RT cells. (A) DSF inhibits the proliferation (green, ***$P < .001$ in both SNU.AT/RT-1 and SNU.AT/RT-2) of ALDH$^+$ AT/RT cells. (B) TUNEL staining shows that DSF increases apoptosis in ALDH$^+$ AT/RT cells (green, ***$P < .001$ in both SNU.AT/RT-1 and SNU.AT/RT-2). The cells were counterstained with DAPI (4′,6′-diamidino-2-phenylindole). Scale bar, 50 μm. (C) Annexin V–stained cells confirmed the early apoptotic cells (***$P < .001$ in SNU.AT/RT-1 and *$P < .05$ in SNU/ATRT-2) and late apoptotic cells (***$P < .001$ in SNU.AT/RT-1 and *$P < .05$ in SNU/ATRT-2). (D) Cell cycle analysis indicates cell cycle G2 arrest (*$P < .05$ in both SNU.AT/RT-1 and SNU.AT/RT-2).

assay. Tumor spheres were not generated or were very small in size after DSF treatment (control vs DSF-treated cells: 23.2 ± 2.5 vs 5.6 ± 1.7, $P < .05$ in SNU.AT/RT-1 and 26.8 ± 3.5 vs 7.5 ± 3.4, $P < .05$ in SNU.AT/RT-2; Fig. 2C and D).

The minimal frequency of repopulating tumor spheres was determined by limiting dilution analysis. DSF-treated cells showed small cell clusters and were difficult to count in the limiting dilution assay (control vs DSF in SNU.AT/RT-1, $P < .001$; in SNU.AT/RT-2, $P < .01$; Fig. 2E).

Inhibition of Proliferation and Induction of Apoptosis and Cell Cycle Arrest by Disulfiram

To investigate the biological function of DSF, we evaluated proliferation, apoptosis, and the cell cycle in ALDH$^+$ AT/RT cells following DSF treatment.

EdU staining indicated that DSF treatment was associated with significantly decreased cell proliferation in ALDH$^+$ AT/RT cells (control vs DSF-treated cells: 67.4% ± 2.0% vs 6.9% ± 2.5%, $P < .001$ in SNU.AT/RT-1 and 73.2% ± 2.8% vs 10.1% ± 4.5%, $P < .001$ in SNU.AT/RT-2; Fig. 3A).

TUNEL staining demonstrated that DSF treatment was associated with significantly accelerated apoptosis compared with the control group (control vs DSF-treated cells: 1.9% ± 1.2% vs 68.1% ± 10.1%, $P < .001$ in SNU.AT/RT-1 and 4.7% ± 2.5% vs 37.1% ± 4.6%, $P < .001$ in SNU.AT/RT-2; Fig. 3B).

The number of early apoptotic cells (annexin V positive and PI negative) in SNU.AT/RT-1 and -2 increased to 12.8% ± 4.2% ($P < .001$) and 5.6% ± 3.8% ($P < .05$), respectively, and the number of late apoptotic cells (necrotic cells: annexin V positive, PI positive) increased to 18.6% ± 2.8% ($P < .001$) and 5.2% ± 4.0% ($P < .05$), respectively, compared with <5% in control cells ($P < .05$; Fig. 3C).

ALDH$^+$ AT/RT cells treated with DSF showed an increased fraction of cells in the G2 phase (control vs DSF-treated cells: 11.8% ± 5.0% vs 16.4% ± 6.4%, $P < .05$ in SNU.AT/RT-1 and 9.1% ± 3.2% vs 16.6% ± 1.9% in SNU.AT/RT-2, $P < .05$; Fig. 3D).

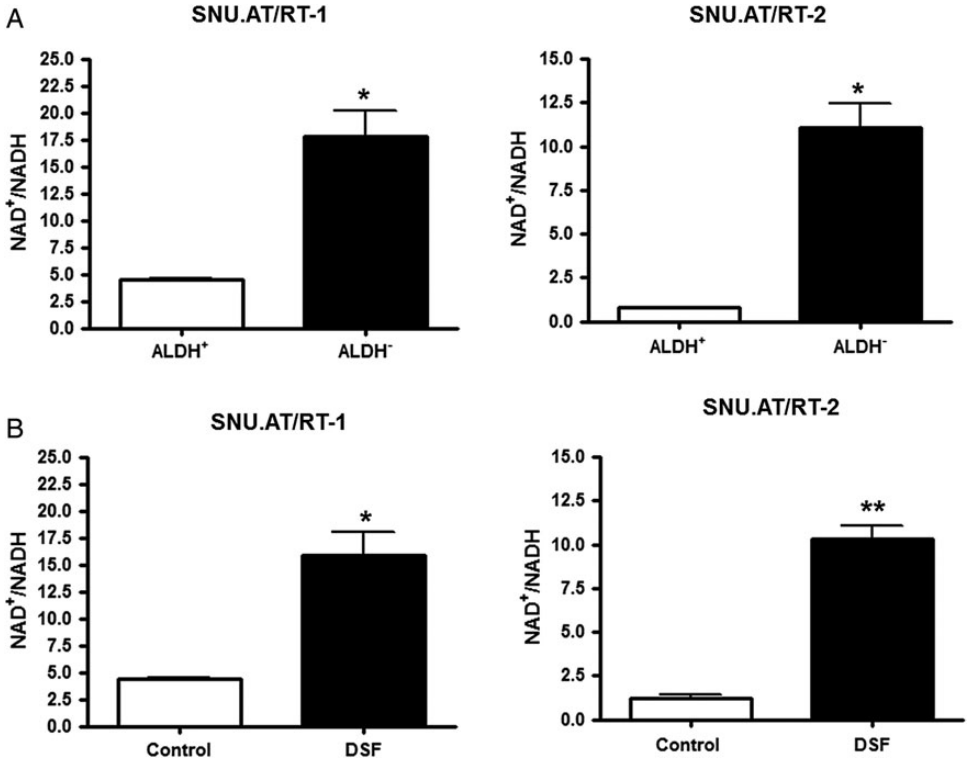

Fig. 4. Metabolic change of AT/RT cells. (A) ALDH$^+$ AT/RT cells have a lower NAD$^+$/NADH ratio than ALDH$^-$ cells (*$P < .05$ in both SNU.AT/RT-1 and SNU.AT/RT-2). (B) ALDH$^+$ AT/RT cells have an increased NAD$^+$/NADH ratio after DSF treatment (*$P < .05$ in SNU.AT/RT-1 and ***$P < .001$ in SNU.AT/RT-2).

Reduced Metabolism by Disulfiram

To identify changes in metabolism, we quantified NAD$^+$/NADH in ALDH$^+$ AT/RT cells after DSF treatment. The inhibition of ALDH by DSF may change the NAD$^+$/NADH equilibrium, thereby affecting enzymatic activities. The ALDH$^+$ AT/RT cells have a low NAD$^+$/NADH ratio compared with ALDH$^-$ AT/RT cells (ALDH$^+$ vs ALDH$^-$: 4.5 ± 0.4 vs 17.8 ± 4.9, $P < .05$ in SNU.AT/RT-1 and 0.8 ± 0.4 vs 11.1 ± 2.4, $P < .05$ in SNU.AT/RT-2; Fig. 4A). Interestingly, the NAD$^+$/NADH ratio was increased (control vs DSF-treated cells: 4.4 ± 0.2 vs 15.9 ± 3.9, $P < .05$ in SNU.AT/RT-1 and 1.2 ± 0.4 vs 10.3 ± 1.3, $P < .01$ in SNU.AT/RT-2; Fig. 4B) by DSF in both ALDH$^+$ AT/RT cells.

Regulation of SIRT1, NF-κB, and Lin28A/B by Disulfiram

To evaluate the possible biological pathway related to the reduced metabolism observed after DSF treatment, we evaluated the levels of SIRT1, NF-κB, Lin28A/B, and miRNA let-7g. The increased NAD$^+$/NADH ratio after DSF treatment induced an upregulation of SIRT1 (Fig. 5A and B). Because SIRT1 inhibits NF-κB expression,[15–17] we measured the level of NF-κB and confirmed its downregulation (Fig. 5A and B). Next, we measured the level of Lin28A/B and miRNA let-7g because NF-κB controls the expression of Lin28A/B,[18,19] and there is a reciprocal expression pattern between Lin28A/B and miRNA let-7g.[20,21] Downregulation of NF-κB resulted in decreased expression of Lin28A/B (Fig. 5A and B) and increased expression of miRNA let-7g in an inverse proportion to Lin28A/B (Fig. 5C). On the other hand, pSTAT3 and pAkt expression were not changed significantly after DSF treatment (Supplementary Fig. S2).

In vivo Therapeutic Effect of Disulfiram in an Atypical Teratoid/Rhabdoid Tumor Mouse Model

The anticancer effect of DSF treatment was confirmed using in vivo studies. We established xenografts of ALDH$^+$ AT/RT cells in immunodeficient nude mice.

Histologic analysis showed a reduction of tumor volume in the brains of DSF-treated mice compared with control mice (control vs DSF-treated group: 19.1 ± 10.5 mm^3 vs 5.3 ± 4.2 mm^3, $P < .05$; Fig. 6A and B).

We next determined biological action of DSF on brain tumor–derived AT/RT spheroid cells staining with ALDH, Ki-67, and caspase-3. DSF treatment decreased the number of cells positive for ALDH (control vs DSF-treated group: $18.4\% \pm 7.4\%$ vs $2.9\% \pm 2.8\%$, $P < .001$; Fig. 6C and D) and Ki-67 (control vs DSF-treated group: $38.6\% \pm 12.3\%$ vs $11.0\% \pm 5.0\%$, $P < .001$; Fig. 6E and F) but increased the number of cells positive for caspase-3 (control vs DSF-treated group: 0.7 ± 1.2 vs 16.1 ± 11.1, $P < .001$; Fig. 6G and H). Long-term median survival data showed that mice treated with DSF survived significantly longer than mice treated with DMSO (control vs DSF-treated group: 91 d vs 105 d, $P = .02$; Fig. 6I). IFO-treated mice showed no survival gain compared with DMSO control (control vs IFO-treated group: 91 d vs 92 d, $P = .90$). The combination of DSF and IFO did not prolong median survival effectively compared with the

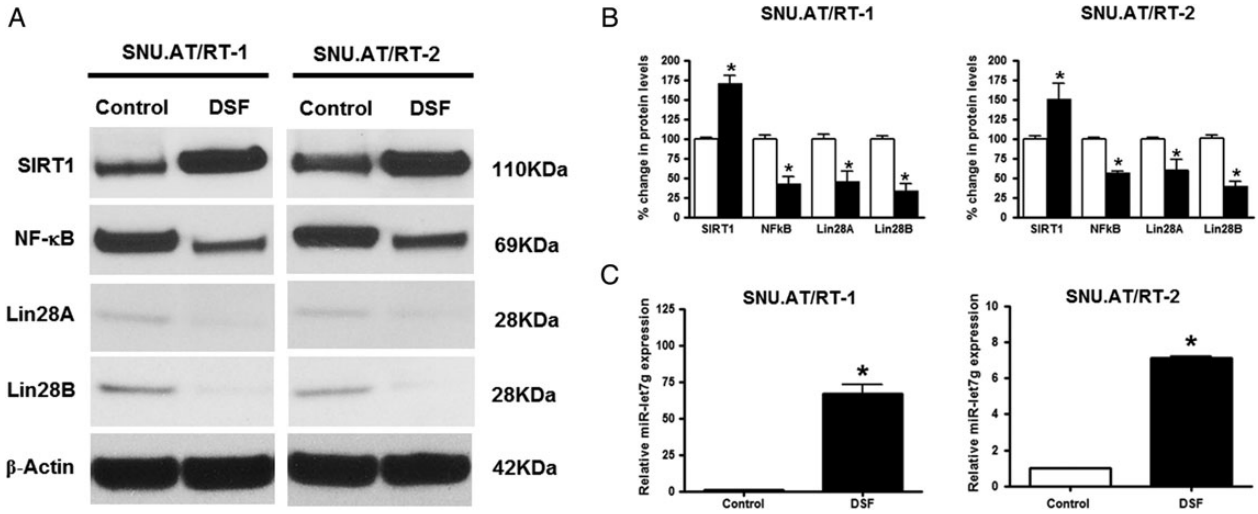

Fig. 5. Signaling pathway of SIRT1, NF-κB, and Lin28A/B after DSF treatment in ALDH$^+$ AT/RT cells. (A and B) Western blot analysis demonstrates that DSF treatment increases SIRT1 protein expression and reduces expression of NF-κB and Lin28A/B in ALDH$^+$ AT/RT cells. (C) Real-time quantitative PCR shows increased expression of miRNA let-7g in ALDH$^+$ AT/RT cells after DSF treatment. *Significant difference from control ($P < .05$).

DSF-only treated group (DSF-treated group vs combination DSF + IFO-treated group: 105 d vs 120 d, $P = .86$). No major systemic toxicities were observed.

Discussion

We isolated cells with high ALDH activity from AT/RT by Aldefluor staining and FACS analysis. We observed an anticancer effect after treating ALDH$^+$ AT/RT cells with DSF using in vitro and in vivo studies. DSF induced changes in metabolism by increasing the NAD$^+$/NADH ratio and regulating SIRT1, NF-κB, Lin28A/B, and miRNA let-7g. Our results show, for the first time, the potential of DSF as an effective chemotherapeutic agent against AT/RT by targeting BTICs.

Recent studies have shown that DSF has an anticancer effect on glioblastoma by compromising stem cell function.[12,13] We have expanded these investigations to determine the therapeutic potential of DSF against AT/RT. In our previous study,[8] we found universal expression of ALDH in primary brain tumors and a higher fraction of ALDH$^+$ cells in aggressive tumors compared with benign tumors. Interestingly, the proportion of ALDH cells within AT/RT was much higher than in glioblastoma (23.50% ± 5.30% in AT/RT vs 4.73% ± 3.30% in glioblastoma).[8] Therefore, the anticancer effect of DSF might be maximally effective in AT/RT through the blockade of ALDH activity.

In the present study, we isolated ALDH$^+$ cells from our patients with AT/RT and found a high expression of ALDH in both tumors (28.8% ± 9.2% in SNU.AT/RT-1 and 18.2% ± 7.2% in SNU.AT/RT-2) in accordance with our previous report. Then, we compared the anticancer effect of DSF with standard anticancer agents, including IFO, carboplatin, and etoposide (ICE regimen), which have been used for conventional chemotherapy against AT/RT.[22] ALDH$^+$ AT/RT cells were more sensitive to DSF than standard anticancer drugs. Notably, standard anticancer drugs demonstrated negligible therapeutic effects against ALDH$^+$ AT/RT cells at physiologically achievable concentrations. DSF treatment effectively decreased ALDH activity and compromised the self-renewal ability of ALDH$^+$ AT/RT cells. The therapeutic potential of DSF was also confirmed in animal studies, exhibiting reduction of tumor volume and significant survival effects.

The anticancer effect of DSF has been suggested to occur through several mechanisms, including the inhibition of DNA methyltransferase activity,[23] proteasomal function,[24] transcription factor, NF-κB[25] and angiogenesis,[26] the induction of intracellular oxidative stress[27] and reactive oxygen species,[13] and the inactivation of the multidrug resistance protein P-glycoprotein.[28] To investigate the possible mechanism of tumor suppression affected by DSF, we focused on the metabolic action of DSF as an ALDH inhibitor. First, we found an increased NAD$^+$/NADH ratio after DSF treatment in AT/RT cells. This increased cellular NAD$^+$ level could intrinsically enhance SIRT1 activity.[29] SIRT1, NAD$^+$-dependent deacetylase sirtuin 1, is a member of the silent information regulator family and has important roles in regulating cell survival, apoptosis, endocrine signaling, cell differentiation, metabolism, chromatin remodeling, and tumorigenesis.[30] Several studies have reported the inhibition of NF-κB transcription following SIRT1 activation,[15–17] which could inhibit Lin28 transcription[18,19] while increasing the miRNA let-7g level.[20,21] Our previous study demonstrated the upregulation of reprogramming-related factors (eg, Lin-28, c-Myc, Krüppel-like factor 4, Sox2) in ALDH$^+$ AT/RT cells.[8] Based on a review of the literature and our previous study, we hypothesized that the SIRT1–NF-κB–Lin28–miRNA let-7g circuitry might be involved in the possible mechanism of the anticancer effects of DSF treatment in AT/RT. This circuitry was confirmed after DSF treatment, resulting in downregulation of Lin28A/B and upregulation of miRNA let-7g.

The combination of DSF with metal, such as copper or zinc, may increase the anticancer effect of DSF.[13] We also confirmed that the combination treatment of DSF with copper showed decreased AT/RT cell viability in vitro. However, cytotoxicity was

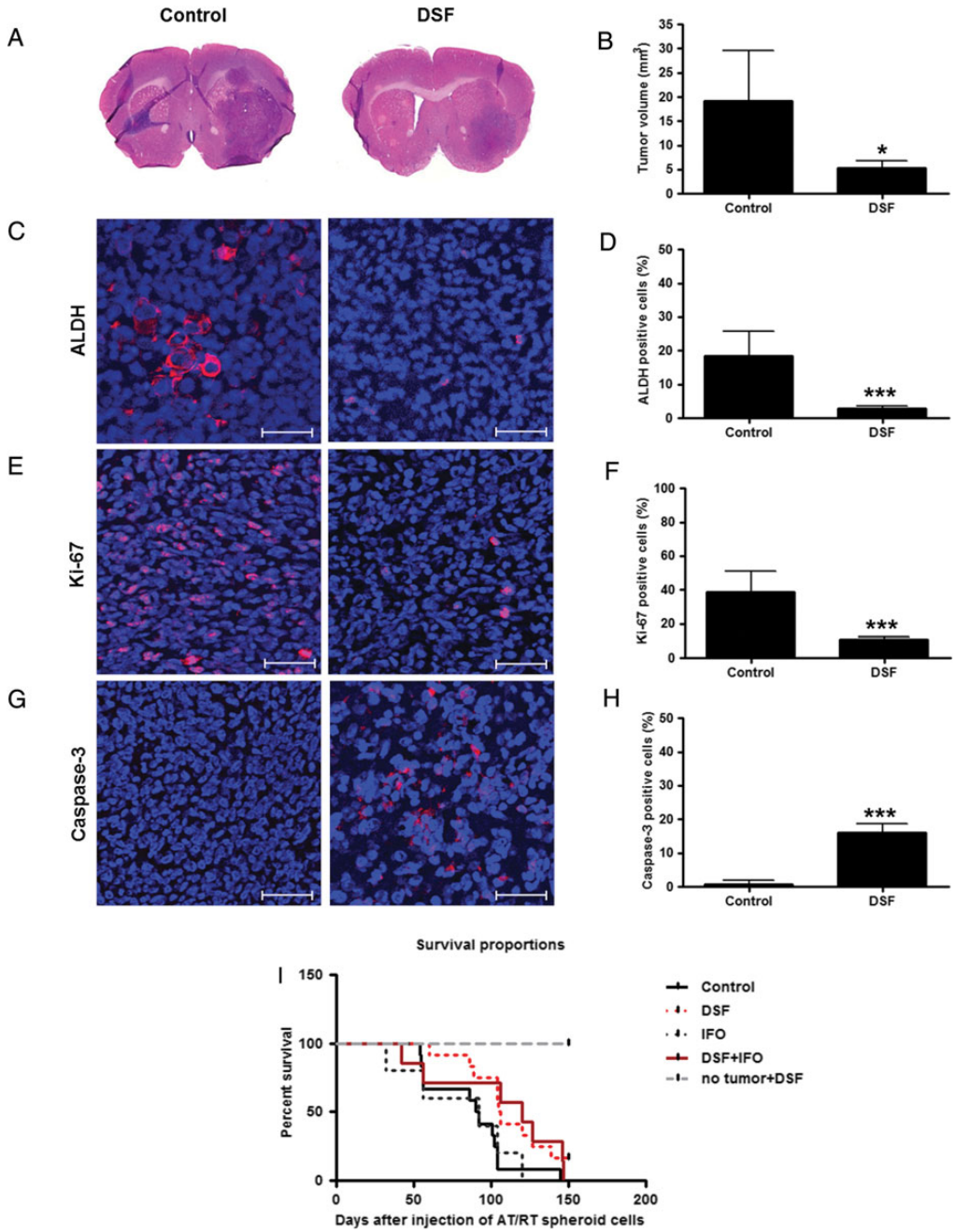

Fig. 6. Therapeutic effect of DSF in vivo. (A and B) Representative histological images show a 42.3% reduction of tumor volume in the brains of DSF-treated mice compared with control mice (*$P < .05$). Hematoxylin and eosin staining. Magnification, 1.25×. (C–H) Representative immunofluorescent images show ALDH (red), Ki-67 (red), caspase-3 (red). By treatment of DSF, ALDH and Ki-67 positive cells were decreased and caspase-3 positive cells were increased (***$P < .001$). Graph shows percentage of positive cells compared with control. Scale bar, 50 μm. Cells were counterstained with 4′,6′-diamidino-2-phenylindole (blue). (I) Kaplan–Meier plots and a log-rank test reveal prolonged survival (105 d) in mice treated with DSF compared with control (91 d, $P = .02$).

enhanced not only in AT/RT cells but also in normal cells such as NSCs (data not shown). Moreover, it is well known that copper and zinc are teratogenic, resulting in neural tube defects.[31] Metals might have a deleterious impact on the genesis of NSCs, especially in young children. We demonstrated that DSF alone, without metal, was also effective in AT/RT treatment. This result might be related to the elevated copper and zinc levels within the tumor cells.[32]

Despite the observed therapeutic efficacy in vivo, complete remission was not achieved. To enhance the therapeutic effect,

combination treatment may be considered, using DSF to target BTICs and standard anticancer drugs to target the bulk tumor cells. However, we could not achieve this goal in the present study. This fact might be due to a lack of effective anticancer drugs against AT/RT at this stage. Another consideration is that DSF may have a narrow therapeutic window and has a cytotoxic effect on not only AT/RT BTICs but also normal cells. Our study showed that the cytotoxic effect on normal cells, such as fibroblasts or NSCs, occurred at a relatively high concentration of DSF, compared with $ALDH^+$ AT/RT cells. However, the optimal dose for DSF should be assessed in the future. Lastly, combination treatment of DSF with radiation might be a viable therapeutic option against AT/RT. We found the possible additive effect of combination treatment with DSF and radiation. This provides a rationale for further evaluation of additive effects of radiotherapy on DSF against AT/RT, including in vivo study.

In conclusion, we demonstrated the therapeutic effects of DSF against BTICs from AT/RT. The effects might be attributed to the modulation of stemness and metabolism. Considering the lack of an effective chemotherapy regimen for AT/RT, DSF may be considered an alternative treatment option against AT/RT.

Supplementary Material

Supplementary material is available at *Neuro-Oncology Journal* online (http://neuro-oncology.oxfordjournals.org/).

Funding

This work was supported by a National Research Foundation of Korea grant funded by the Korean government (MEST) (2012011770) and the Seoul National University Hospital Research Fund (03–2012-0200).

Conflicts of interest statement. None declared.

References

1. Tekautz TM, Fuller CE, Blaney S, et al. Atypical teratoid/rhabdoid tumors (ATRT): improved survival in children 3 years of age and older with radiation therapy and high-dose alkylator-based chemotherapy. *J Clin Oncol*. 2005;23(7):1491–1499.
2. Lee JY, Kim IK, Phi JH, et al. Atypical teratoid/rhabdoid tumors: the need for more active therapeutic measures in younger patients. *J Neurooncol*. 2012;107(2):413–419.
3. Nicolaides T, Tihan T, Horn B, et al. High-dose chemotherapy and autologous stem cell rescue for atypical teratoid/rhabdoid tumor of the central nervous system. *J Neurooncol*. 2010;98(1):117–123.
4. Bernstein KD, Sethi R, Trofimov A, et al. Early clinical outcomes using proton radiation for children with central nervous system atypical teratoid rhabdoid tumors. *Int J Radiat Oncol*. 2013;86(1):114–120.
5. Chen R, Nishimura MC, Bumbaca SM, et al. A hierarchy of self-renewing tumor-initiating cell types in glioblastoma. *Cancer cell*. 2010;17(4):362–375.
6. Bao S, Wu Q, McLendon RE, et al. Glioma stem cells promote radioresistance by preferential activation of the DNA damage response. *Nature*. 2006;444(7120):756–760.
7. Ginestier C, Hur MH, Charafe-Jauffret E, et al. ALDH1 is a marker of normal and malignant human mammary stem cells and a predictor of poor clinical outcome. *Cell Stem Cell*. 2007;1(5):555–567.
8. Choi SA, Lee JY, Phi JH, et al. Identification of brain tumour initiating cells using the stem cell marker aldehyde dehydrogenase. *Eur J Cancer*. 2014;50(1):137–149.
9. Sauna ZE, Shukla S, Ambudkar SV. Disulfiram, an old drug with new potential therapeutic uses for human cancers and fungal infections. *Mol Biosyst*. 2005;1(2):127–134.
10. Chen D, Cui QZC, Yang HJ, et al. Disulfiram, a clinically used anti-alcoholism drug and copper-binding agent, induces apoptotic cell death in breast cancer cultures and xenografts via inhibition of the proteasome activity. *Cancer Res*. 2006;66(21):10425–10433.
11. Wang WG, McLeod HL, Cassidy J. Disulfiram-mediated inhibition of NF-kappa B activity enhances cytotoxicity of 5-fluorouracil in human colorectal cancer cell lines. *Int J Cancer*. 2003;104(4):504–511.
12. Triscott J, Lee C, Hu KJ, et al. Disulfiram, a drug widely used to control alcoholism, suppresses self-renewal of glioblastoma and overrides resistance to temozolomide. *Oncotarget*. 2012;3(10):1112–1123.
13. Liu P, Brown S, Goktug T, et al. Cytotoxic effect of disulfiram/copper on human glioblastoma cell lines and ALDH-positive cancer-stem-like cells. *Brit J Cancer*. 2012;107(9):1488–1497.
14. Choi SA, Wang KC, Phi JH, et al. A distinct subpopulation within CD133 positive brain tumor cells shares characteristics with endothelial progenitor cells. *Cancer Lett*. 2012;324(2):221–230.
15. Yeung F, Hoberg JE, Ramsey CS, et al. Modulation of NF-kappaB-dependent transcription and cell survival by the SIRT1 deacetylase. *EMBO J*. 2004;23(12):2369–2380.
16. Cao L, Liu C, Wang F, et al. SIRT1 negatively regulates amyloid-beta-induced inflammation via the NF-kappaB pathway. *Braz J Med Biol Res*. 2013;46(8):659–669.
17. Kauppinen A, Suuronen T, Ojala J, et al. Antagonistic crosstalk between NF-kappa B and SIRT1 in the regulation of inflammation and metabolic disorders. *Cell Signal*. 2013;25(10):1939–1948.
18. Iliopoulos D, Hirsch HA, Struhl K. An epigenetic switch involving NF-kappaB, Lin28, let-7 microRNA, and IL6 links inflammation to cell transformation. *Cell*. 2009;139(4):693–706.
19. Wang DJ, Legesse-Miller A, Johnson EL, et al. Regulation of the let-7a-3 promoter by NF-kappaB. *PloS One*. 2012;7(2):e31240.
20. Lightfoot HL, Bugaut A, Armisen J, et al. A LIN28-dependent structural change in pre-let-7 g directly inhibits dicer processing. *Biochemistry*. 2011;50(35):7514–7521.
21. Viswanathan SR, Daley GQ. Lin28: a microRNA regulator with a macro role. *Cell*. 2010;140(4):445–449.
22. Fidani P, De Ioris MA, Serra A, et al. A multimodal strategy based on surgery, radiotherapy, ICE regimen and high dose chemotherapy in atypical teratoid/rhabdoid tumours: a single institution experience. *J Neurooncol*. 2009;92(2):177–183.
23. Lin JQ, Haffner MC, Zhang YG, et al. Disulfiram is a DNA demethylating agent and inhibits prostate cancer cell growth. *Prostate*. 2011;71(4):333–343.
24. Hothi P, Martins TJ, Chen LP, et al. High-throughput chemical screens identify disulfiram as an inhibitor of human glioblastoma stem cells. *Oncotarget*. 2012;3(10):1124–1136.

25. Zanotto A, Braganhol E, Schroder R, et al. NF kappa B inhibitors induce cell death in glioblastomas. *Biochem Pharmacol*. 2011; 81(3):412–424.

26. Marikovsky M, Nevo N, Vadai E, et al. Cu/Zn superoxide dismutase plays a role in angiogenesis. *Int J Cancer*. 2002;97(1):34–41.

27. Cen DZ, Gonzalez RI, Buckmeier JA, et al. Disulfiram induces apoptosis in human melanoma cells: a redox-related process. *Mol Cancer Ther*. 2002;1(3):197–204.

28. Loo TW, Bartlett MC, Clarke DM. Disulfiram metabolites permanently inactivate the human multidrug resistance P-glycoprotein. *Mol Pharm*. 2004;1(6):426–433.

29. Canto C, Gerhart-Hines Z, Feige JN, et al. AMPK regulates energy expenditure by modulating NAD+ metabolism and SIRT1 activity. *Nature*. 2009;458(7241):1056–1060.

30. Michan S, Sinclair D. Sirtuins in mammals: insights into their biological function. *Biochem J*. 2007;404:1–13.

31. Zeyrek D, Soran M, Cakmak A, et al. Serum copper and zinc levels in mothers and cord blood of their newborn infants with neural tube defects: a case-control study. *Indian Pediatr*. 2009;46(8):675–680.

32. Rizk SL, Skypeck HH. Comparison between concentrations of trace-elements in normal and neoplastic human-breast tissue. *Cancer Res*. 1984;44(11):5390–5394.